Synthesis of Supported Single-Crystalline Organic Nanowires by Physical Vapor Deposition

Ana Borras,*[,†] Myriam Aguirre,[‡] Oliver Groening,[†] Carlos Lopez-Cartes,[§] and Pierangelo Groening[†]

"nanotech@surfaces" Laboratory, Empa, Swiss Federal Laboratories for Materials Testing and Research, Feuerwerkerstrasse 39, CH-3602 Thun, Switzerland, "Solid State Chemistry and Analysis" Laboratory, Überlandstrasse 129, CH-8600 Dübendorf, Switzerland, and ICMSE (CSIC-Universidad de Sevilla), Avenida Americo Vespucio s/n, 41092 Sevilla, Spain

Received August 8, 2008
Revised Manuscript Received October 30, 2008

Functional one-dimensional (1D) materials are of great interest for their use in nanoscale devices. Historically, more efforts have been focused on carbon and inorganic nanostructures[1] than on their organic semiconductor counterparts.[2] However, during the last years, the interest in porphyrins and phthalocyanines as building blocks for organic nanostructures has been increasing. Because of their desirable optical, electrical, and catalytic properties,[3] these organic semiconductor dyes are promising materials in applications such as vapor nanosensors and as active components for photonic devices, organic field effect transistors (OFETs), phototransistors, and solar cells.[3d,e,4] Porphyrin and phthalocyanine 1D-semiconducting nanostructures have been synthesized by different strategies most of them comprising 1D dimensional self-assembly via solution deposition[5] or physical vapor transport.[6] In this work, we show a novel method for growing supported organic semiconductor nanowires by a vapor transport deposition process. We report the production of high-density supported porphyrin and phthalocyanine nanowire films on flat substrates coated by a thin silver oxide layer. By the sequential synthesis of these two types of nanowires on the same substrate a novel type of open core@shell heterostructure is obtained. Although further investigations are underway to elucidate the growth mechanism and carry out the optical and electrical characteristics of these nanowires, the aim of this work is to demonstrate the versatility of this synthetic approach and their generalization to different porphyrin and phthalocyanine molecules for the deposition of organic semiconductor nanowires and open core@shell heterostructures.

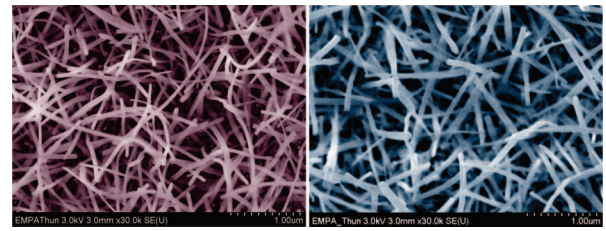

Figure 1. Planar view SEM micrographs of the (left) PtOEP and (right) CuPc nanowires on the oxidized Ag/silicon substrates.

Until now, we have successfully synthesized different 1D-nanostructures including octaethyl porphyrin (OEP), platinum and palladium octaethyl porphyrins (PtOEP and PdOEP), and copper phthalocyanine (CuPc) nanowires (see Scheme 1 in the Supporting Information. Experimental details are also included in this section). The key parameters for the synthesis of these nanowires are both the substrate temperature and the presence of silver oxide nanoparticles on the flat silicon substrates. The sublimation of the dye molecules in argon at 0.020 mbar on these heterogeneous substrates results in the growth of a high density nanowire film, as it is shown in Figure 1 (see also Figure S1 of the Supporting Information). Films with nanowires densities as high as $\sim 1 \times 10^9$ per cm^{-2} and nanowire growth rates of up to 0.5 μm min^{-1} can be obtained by this methodology. The substrate temperature during the deposition was maintained at 140 ± 5 °C for the PtOEP (Figure 1, left) and at 220 ± 5 °C for the CuPc (Figure 1, right). The preferential formation of nanowires instead of other aggregates, such as micrometer rods, is achieved whenever the temperature of the composite substrates (T_{subs}) and the sublimation temperature of the dye in the Ar atmosphere (T_S) complies with the expression: $T_{subs} > 0.7T_S$. Furthermore, we observed that silver oxide nanoparticles act as an effective promoter for the formation of these nanowires. An in deep analysis of the silver oxidation state on Si substrates can be found elsewhere.[7]

* Corresponding author.
† EMPA, Swiss Federal Laboratories for Materials Testing and Research nanotech@surfaces.
‡ EMPA, Swiss Federal Laboratories for Materials Testing and Research, Solid State Chemistry and Analysis.
§ ICMSE (CSIC-Universidad de Sevilla).

(1) (a) Xia, Y. N.; Yang, P. D.; Sun, Y. G.; Wu, Y. Y.; Mayers, B.; Gates, B.; Yin, Y. D.; Kim, F.; Yan, Y. Q. *Adv. Mater.* **2003**, *15*, 353. (b) Rao, C. N. R.; Deepak, F. L.; Gundiah, G.; Govindaraj, A. *Prog. Solid State Chem.* **2003**, *31*, 5.
(2) Schenning, A. P. H. J.; Meijer, E. W. *Chem. Commun.* **2005**, 3245.
(3) (a) Kwong, R. C.; Sibley, S.; Dubovoy, T.; Baldo, M.; Forrest, S. R.; Thompson, M. E. *Chem. Mater.* **1999**, *11*, 3709. (b) Armstrong, N. R. *J. Porphyrins Phthalocyanines* **2000**, *4*, 414. (c) Spadavecchia, J.; Ciccarella, G.; Rella, R.; Capone, S.; Siciliano, P. *Chem. Mater.* **2004**, *16*, 2083. (d) Claessens, C. G.; Hahn, U.; Torres, T. *Chem. Rec.* **2008**, *8*, 75. (e) Troshin, P. A.; Koeppe, R.; Peregudov, A. S.; Peregudova, S. M.; Egginger, M.; Lyubovskaya, R. N.; Sariciftci, N. S. *Chem. Mater.* **2007**, *19*, 5363. (f) Sorokin, A. B.; Tuel, A. *Catal. Today* **2000**, *57*, 45. (g) Curtis, M. D.; Cao, J.; Kampf, J. W. *J. Am. Chem. Soc.* **2004**, *126*, 4318. (h) Kang, S. W.; Li, Q.; Chapman, B. D.; Pindak, R.; Cross, J. O.; Li, L. F.; Nakata, M.; Kumar, S. *Chem. Mater.* **2007**, *19*, 5657. (i) Lei, S. B.; Yin, S. X.; Wang, C.; Wan, L. J.; Bai, C. L. *Chem. Mater.* **2002**, *14*, 2837.
(4) (a) Tang, Q.; Li, H.; Liu, Y.; Hu, W. *J. Am. Chem. Soc.* **2006**, *128*, 14634. (b) Rakow, A. N.; Suslick, K. S. *Nature* **2000**, *17*, 710.
(5) (a) Wang, Z.; Medforth, C. J.; Shelnutt, J. A. *J. Am. Chem. Soc.* **2004**, *126*, 15954. (b) Schwab, A. D.; Smith, D. E.; Rich, C. S.; Young, E. R.; Smith, W. F.; de Paula, J. C. *J. Phys. Chem. B* **2003**, *107*, 11339. (c) Sostaric, J. Z.; Pandian, R. P.; Weavers, L. K.; Kuppusamy, P. *Chem. Mater.* **2006**, *18*, 4183. (d) Kojima, T.; Harada, R.; Nakanishi, T.; Kaneko, K.; Fukuzumi, S. *Chem. Mater.* **2007**, *19*, 51.
(6) (a) Tang, Q.; Li, H.; Song, Y.; Hu, W.; Jiang, L.; Liu, Y.; Wang, X.; Zhu, D. *Adv. Mater.* **2006**, *18*, 3010. (b) Tong, W. Y.; Djurisic, A. B.; Ng, A. M. C.; Chan, W. K. *Thin Solid Films* **2007**, *515*, 5270. (c) Xiao, K.; Tao, J.; Pan, Z.; Puretzky, A. A.; Ivanov, I. N.; Pennycook, S. J.; Geohegan, D. B. *Angew. Chem.* **2007**, *119*, 2704. (d) Mbenkum, B. N.; Barrena, E.; Zhang, X.; Kelsch, M.; Dosch, H. *Nano Lett.* **2006**, *12*, 2852. (e) Barrena, E.; Zhang, X. N.; Mbenkum, B. N.; Lohmueller, T.; Krauss, T. N.; Kelsh, M.; van Aken, P. A.; Spatz, J. P.; Dosh, H. *ChemPhysChem* **2008**, *9*, 1114.

10.1021/cm802172p CCC: $40.75 © 2008 American Chemical Society
Published on Web 11/17/2008

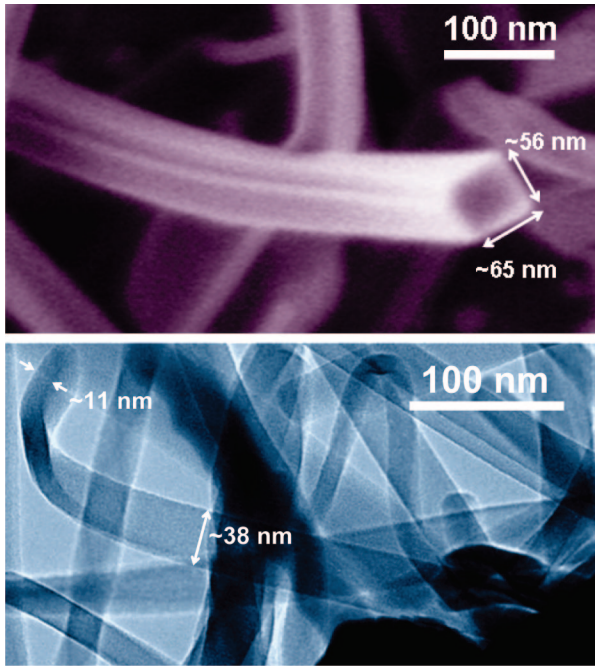

Figure 2. (Top) High-magnification SEM image of a squared PtOEP nanowire. (Bottom) TEM microghaph of a CuPc nanobelt showing details of the nanowire shape and dimension.

The nanowires grow from the oxidized Ag/Si surface following a rectangular shape footprint with a regular cross section over the whole length of the wires. When the deposition process is carried out at T_{subs} closed to $0.7T_S$, the morphology of the wires can be broadly divided in two groups. The difference between these two sets of nanowires is the aspect ratio of their footprints from almost flat to squared nanowires. The micrographs in Figure 2 show a characteristic nanowire corresponding to the squared group (Figure 2, top) and to the higher-aspect-ratio cross-section family (Figure 2, bottom). The widths of the flat nanowires or nanobelts are in the range from 20 to 150 nm, with aspect ratios as high as 4. For the squared nanowires, the widths vary between 40 and 75 nm. In both cases, nanowires with lengths between 0.2 and 5 μm can be grown depending mostly on the deposition time. On the other hand, the nanowires present a high flexibility as it is easily demonstrated by their ability to turn and bend under electron beam irradiation (see Figure S2 in the Supporting Information). In fact, the nanobelts present more complex movements and turns than the squared wires, including wrapping actions. This behavior hinders the characterization of the nanowires. However, it is a crucial factor in the formation of the open core@shell structure as it is discussed below. The nanowire shape, length, and thickness, as well as the wire density, can be controlled adjusting the experimental parameters. Although at $T_{sust} \approx 0.7T_S$, the amount of belt-shaped and squared nanowires are similar, the increase in T_{subs} ($T_{subs} > 0.90T_S$) causes the preferential formation of the latter group, being generally thinner and longer (see Figure S3 in the Supporting Information).

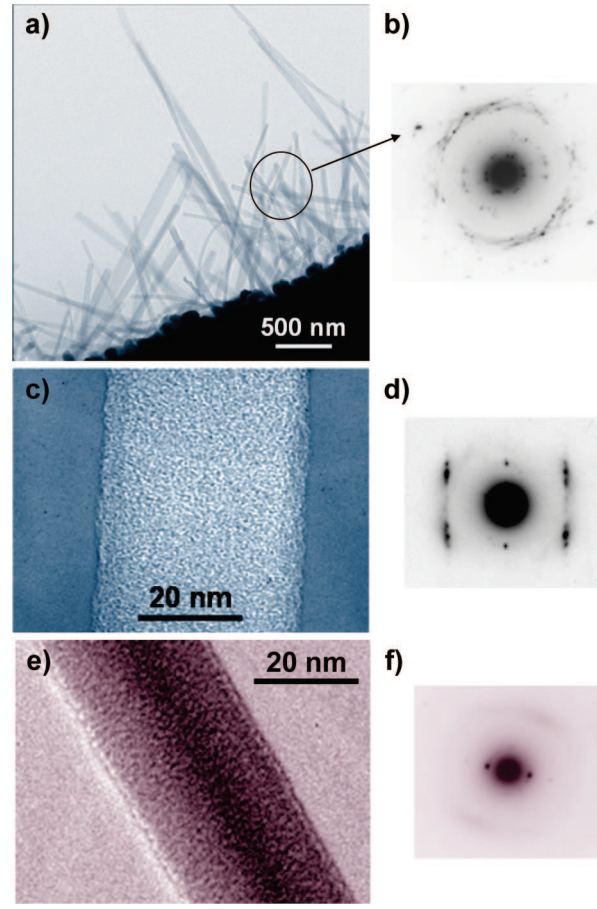

Figure 3. TEM image of (a) the CuPc nanowire coating and the representative HRTEM image of (c) a belt-shape CuPc and (e) squared PtOEP nanowires. (b, d, f) Corresponding selected area electron diffraction (SAED) patterns. Note that the amorphization under the electron beam causes the distortion of the patterns.

The structural characterization of the nanowires was carried out by transmission electron microscopy (TEM) and selected area electron diffraction (SAED) (Figure 3). From Figure 2 and the high-resolution images of individual nanowire in images c and d in Figure 3 as well as from EDX (see Figure S4 in the Supporting Information), it is concluded that no Ag particles are incorporated into the organic nanowires. On the other hand, the SAED spectra in Figure 3b for a randomly oriented set of nanowires and for a single CuPc nanobelt (Figure 3d) and a PtOEP squared nanowire (Figure 3f) reveal that the porphyrin and phthalocyanine nanowires are single-crystalline. This result agrees with the development of 1D phthalocyanine nanostructures reported in the literature in other systems.[4a,6a,b] The absence of Ag particles in the nanowire, in particularly on its apex, and the formation of single-crystalline nanowires indicate that the classic vapor−liquid−solid (VLS) growth mechanism of 1D nanostructure can be rejected in favor of a crystallization process. This mechanism implying preferential diffusion of the porphyrin and phthalocyanine molecules arriving on the substrate through the oxidized Ag particle, with a estimated

(7) (a) Bielmann, M.; Schwaller, P.; Ruffieux, P.; Groening, O.; Schlapbach, L.; Groening, P. *Phys. Rev. B* **2002**, *65*, 235431. (b) Borras, A.; Barranco, A.; Yubero, F.; Gonzalez-Elipe, A. R. *Nanotechnology* **2006**, *17*, 3518. (c) Borras, A.; Barranco, A.; Espinos, J. P.; Cotrino, J.; Holgado, J. P.; Gonzalez-Elipe, A. R. *Plasma Processes Polym.* **2007**, *4*, 515.

(8) (a) Drager, A. S.; Zangmeister, R. A. P.; Armstrong, N. R. *J. Am. Chem. Soc.* **2001**, *123*, 3595. (b) Xiao, S.; Tang, J.; Beetz, T.; Guo, X.; Tramblay, N.; Siegrist, T.; Zhu, Y.; Steigewald, M.; Nuckolls, C. *J. Am. Chem. Soci.* **2006**, *128*, 10700. (c) Lee, W. H.; Kim, D. H.; Jang, Y.; Cho, J. H.; Hwang, M.; Park, Y. D. *Appl. Phys. Lett.* **2007**, *90*, 132106.

flux of ~2000 mol s^{-1}, indicating a highly dynamic growth process undergoing a liquid−solid phase transition at the nucleation site. Thus, the most promising explanation to the formation of these 1D-nanostructures rests on the formation of crystals by self-assembly of these molecules along the wire axe via strong $\pi-\pi$ interactions, being the nucleation sites the silver particles. A clear advantage of our methodology is that the oxidized silver particles act as nucleation sites for both porphyrins and phthalocyanines nanowires. Thus, such 1D nanostructures can be grown on flat surfaces (i.e., Si(100) wafers)n not necessary highly rough surfaces as in recent examples in the literature on phthalocyanine nanowires.[6b] On the other hand, the growth of phthalocyanine nanowires on metal substrates has also been studied lately.[6c−e] Xiao et al.[6c] have reported the formation of copper-tatracyanoquinodimethane (Cu-TCNQ) nanowires by deposition of TCNQ on a Cu thin film. By this process, the TCNQ vapor reacts chemically with the Cu surface, providing the formation of single-crystal conical nanowires. Such a chemical reaction yields the formation of Cu-TCNQ nanowires but does not represent a route for the formation the porphyrin nanowires. In the same way, Barrena et al.[6d,e] have shown the growth of F_{16}CuPc nanotubes and non crystalline nanofibers on gold particles by a base-growth mechanism. Therefore, it is worth remarking that the crystallization process summarized herein represents the first general method for the formation of both porphyrin and phthalocyanine crystalline nanowires and nanobelts.

This one step method presents significant advantages for the synthesis of porphyrin and phthalocyanine nanowires such its simplicity, mild conditions, relative low substrate temperature, as well as the high homogeneity and crystallinity of the nanowires synthesized. Nevertheless, the most interesting characteristic of this novel methodology is the possibility of growing simultaneously nanowires formed by different molecules.

Figure 4 shows some results of the combination of the two immiscible molecules PtOEP and CuPc during the deposition. In this experiment the growth of the nanowires was sequential, starting with the CuPc evaporation at T_{subs} of 220° ± 5 °C, a temperature at which one of the predominant morphologies for the CuPc nanostructures is as nanobelts. The PtOEP was added after the formation of the CuPc nanobelts at T_{subs} of 170° ± 5 °C. For the latter T_{subs}, the PtOEP formed squared nanowires with a thickness varying between 15 and 30 nm (Figure S3). Following this procedure an open core@shell architecture, PtOEP@CuPC formed by a PtOEP inner wire enveloped in a CuPc outer belt is obtained (See Figures S5 for EDX analysis and Figure S6). The number of these open core@shell nanowires depends on the density of both, the PtOEP nanowires and CuPc nanobelts, and the number of nucleation sites. After a thoroughly analysis by SEM and TEM and taking into account the high flexibility of the nanowires, it is possible to elucidate that the CuPc nanobelts are wrapped along their axis embracing the PtOEP squared nanowires from their base (see Figures 4 c) and Figure S7) forming an open core@shell heterostructure. As far as we know this is the first example

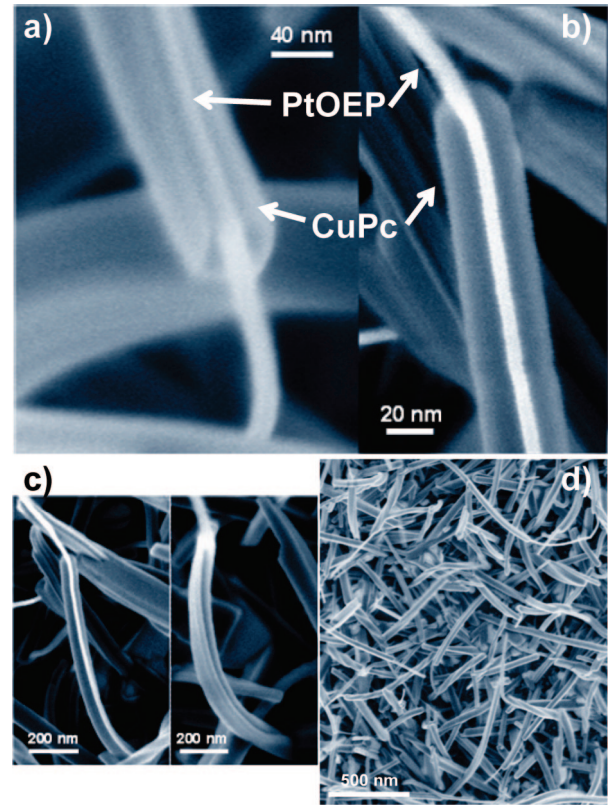

Figure 4. (a−c) High-magnification SEM micrographs of the open core@shell nanowires. The more brilliant contrast of the inner wire respect to the shell is due to the difference in atomic number between Pt and Cu. A high density of such heterostructures is shown in (d).

in the literature where this type of 1D-dimensional, coaxial, organic hereterostructure has been shown. An intense experimental work is under progress to determine the properties of these open core@shell nanowires and possible applications. These results will be presented in a forthcoming article. The present results demonstrate the possibility to form a new type of heterostructured nanowires by tuning the molecules arriving to the surface during the nanowire growth. This methodology can be of the upmost interest for the synthesis of novel n-p nanowires junction of interest for solar energy harvesting applications.[3i] The face-to-face staking is common in planar aromatic molecules such as metal porphyrins and phthalocyanines, hexabenzocoronene and pentacene derivatives.[8] Therefore, although we have focused this work in the growth of OEP, metal OEP and CuPc, its extrapolation to other systems presenting π stacking is also promising.

Acknowledgment. We acknowledge the EU for financial support (PHODYE STREP Project Contract 033793). We thank G. Buerki (EMPA) and T. C. Rojas (ICMSE) for their assistance during SEM and TEM characterization.

Supporting Information Available: Experimental details and additional characterizations (PDF). This information is available free of charge via the Internet at http://pubs.acs.org.

CM802172P